RESEARCH BRIEF

Activating *ESR1* Mutations Differentially Affect the Efficacy of ER Antagonists

Weiyi Toy[1], Hazel Weir[2], Pedram Razavi[1,3], Mandy Lawson[2], Anne U. Goeppert[4], Anne Marie Mazzola[5], Aaron Smith[2], Joanne Wilson[2], Christopher Morrow[2], Wai Lin Wong[6], Elisa De Stanchina[6], Kathryn E. Carlson[7], Teresa S. Martin[7], Sharmeen Uddin[1], Zhiqiang Li[1], Sean Fanning[8], John A. Katzenellenbogen[7], Geoffrey Greene[8], José Baselga[1,3,9], and Sarat Chandarlapaty[1,3,9]

ABSTRACT

Recent studies have identified somatic *ESR1* mutations in patients with metastatic breast cancer and found some of them to promote estrogen-independent activation of the receptor. The degree to which all recurrent mutants can drive estrogen-independent activities and reduced sensitivity to ER antagonists like fulvestrant is not established. In this report, we characterize the spectrum of *ESR1* mutations from more than 900 patients. *ESR1* mutations were detected in 10%, with D538G being the most frequent (36%), followed by Y537S (14%). Several novel, activating mutations were also detected (e.g., L469V, V422del, and Y537D). Although many mutations lead to constitutive activity and reduced sensitivity to ER antagonists, only select mutants such as Y537S caused a magnitude of change associated with fulvestrant resistance *in vivo*. Correspondingly, tumors driven by Y537S, but not D5358G, E380Q, or S463P, were less effectively inhibited by fulvestrant than more potent and bioavailable antagonists, including AZD9496. These data point to a need for antagonists with optimal pharmacokinetic properties to realize clinical efficacy against certain *ESR1* mutants.

SIGNIFICANCE: A diversity of activating *ESR1* mutations exist, only some of which confer resistance to existing ER antagonists that might be overcome by next-generation inhibitors such as AZD9496. *Cancer Discov; 7(3); 277–87. ©2016 AACR.*

INTRODUCTION

Therapeutic targeting of estrogen synthesis is a mainstay of therapy for the over 70% of breast cancers that feature estrogen receptor expression. These treatments markedly reduce the risk of recurrence from early-stage disease and improve outcomes in those with advanced disease (1, 2).

Despite this efficacy, a significant subset of estrogen receptor–positive (ER^+) breast tumors ultimately develops resistance to antiestrogen therapy. Recent work has identified a set of recurrent mutations in the estrogen receptor *ESR1* from patients with hormone-refractory metastatic breast cancer (MBC; refs. 3–7). These analyses from small populations of patients

[1]Human Oncology and Pathogenesis Program, Memorial Sloan Kettering Cancer Center, New York, New York. [2]AstraZeneca, iMED Oncology, Cambridge, UK. [3]Breast Medicine Service, Department of Medicine, Memorial Sloan Kettering Cancer Center, New York, New York. [4]AstraZeneca, Discovery Sciences, IMED Biotech Unit, Cambridge, UK. [5]AstraZeneca, iMED Oncology, Waltham, Massachusetts. [6]Antitumor Assessment Core, Memorial Sloan Kettering Cancer Center, New York, New York. [7]Department of Chemistry, University of Illinois at Urbana-Champaign, Urbana, Illinois. [8]Ben May Department for Cancer Research, University of Chicago, Chicago, Illinois. [9]Weill Cornell Medical College, New York, New York.

Note: Supplementary data for this article are available at Cancer Discovery Online (http://cancerdiscovery.aacrjournals.org/).

Corresponding Author: Sarat Chandarlapaty, Memorial Sloan Kettering Cancer Center, 1275 York Avenue, New York, NY 10065. Phone: 646-888-3387; Fax: 646-888-3406; E-mail: chandars@mskcc.org

doi: 10.1158/2159-8290.CD-15-1523

described mutations within the ligand-binding domain (LBD) of the receptor, with the majority of the mutations at residues Y537 and D538. It was not clear whether a greater repertoire of somatic LBD mutants might be identified by sequencing a larger population of MBCs. Recurrent mutations at Y537 and D538 were characterized using biochemical, cellular, and structural analyses and were shown to promote (i) an aporeceptor conformation similar to that of an estradiol-bound receptor, (ii) constitutive coactivator binding and transcriptional activity in the absence of estrogen, and (iii) hormone-independent proliferation when expressed in hormone-dependent cells (3, 8, 9). Also evident from these studies was the potential for ER antagonists to potently inhibit mutant receptor activities. However, whether existing antagonists had sufficient potency and adequate pharmacokinetic properties to inhibit mutant receptors *in vivo* and thereby overcome hormone-resistant phenotypes has not been clear.

In this study, we analyzed *ESR1* DNA sequences from a large series of metastatic breast tumors and found several novel LBD mutations that constitutively activate the receptor and promote breast cancer phenotypes. We further investigated the ability of ER antagonists to potently inhibit mutant receptor activities. We observed differential sensitivity of the LBD mutants to selective estrogen receptor degraders (SERD). Among the mutants Y537S was the most constitutively active and required the highest drug concentrations to fully inhibit the receptor. This specific mutant proved to be less effectively antagonized *in vivo* by fulvestrant, a drug with suboptimal pharmacokinetic properties compared with the more potent and orally bioavailable SERD AZD9496. Collectively, these data suggest that activating *ESR1* LBD mutations differentially affect the efficacy of ER antagonists.

RESULTS

Novel *ESR1* LBD Mutations in Patients with Hormone-Resistant Breast Cancer

With an expansion of our efforts to analyze mutations present in MBC using next-generation sequencing (National Clinical Trials Registry #00897702), we now have a more comprehensive portrait of the diversity and frequency of *ESR1* mutations in MBC (Fig. 1A). In this series, over 929 cases of breast cancer (including ER^+, $HER2^+$, and ER^- tumors) were analyzed, with 95 patients having somatic mutations in *ESR1* (Table 1). Somatic mutations were found in the LBD in all but one case. Clinically, 85 out of 95 patients with *ESR1* mutations had $ER^+/HER2^-$ MBC, whereas 10 of them were $ER^+/HER2^+$. In terms of treatment in the metastatic setting, 67.4% of the *ESR1*-mutant patients had prior exposure to an aromatase inhibitor (AI), whereas only 18.8% of the wild-type (WT) patients had an AI as a treatment for metastatic disease (Supplementary Table S1). Among the metastatic sites with *ESR1* mutations detected,

Table 1. Clinical characteristics of the tumor biopsies sequenced in the study

Characteristics	Total, $N = 929$	*ESR1* WT, $N = 834$	*ESR1* mutated, $N = 95$	*P*
Receptor subtype				
$HR^+/HER2^-$	139	546 (86.5%)	85 (13.5%)	
$HR^+/HER2^+$	126	116 (92.1%)	10 (7.9%)	
$HR^-/HER2^+$	50	50 (100%)	0 (0%)	
Triple negative	122	122 (100%)	0 (0%)	<0.00001
Histology				
Invasive ductal	698	626 (89.7%)	72 (10.3%)	
Invasive lobular	141	121 (85.8%)	20 (14.2%)	
Mixed ductal/lobular	42	42 (100%)	0 (0%)	
Carcinoma NOS	38	35 (92.1%)	3 (7.9%)	
Other	10	10 (100%)	0 (0%)	0.09
Site of biopsy				
Primary	313	302 (96.5%)	11 (3.5%)	
Metastasis	616	532 (86.4%)	84 (13.6%)	<0.00001
Metastatic site biopsied ($N = 616$)				
Liver	160	126 (78.8%)	34 (21.3%)	
Lymph node	96	90 (93.8%)	6 (6.3%)	
Bone	89	79 (88.8%)	10 (11.2%)	
Chest wall	53	46 (86.8%)	7 (13.2%)	
Lung	49	45 (91.8%)	4 (8.2%)	
Brain	24	24 (100%)	0 (0%)	
Soft tissue	25	22 (88%)	3 (12%)	
Ovary	22	21 (95.5%)	1 (4.5%)	
Skin	24	21 (87.5%)	3 (12.5%)	
Pleura	23	20 (87%)	3 (13%)	
Other	51	38 (74.5%)	13 (25.5%)	0.0017

Abbreviation: NOS, not otherwise specified.

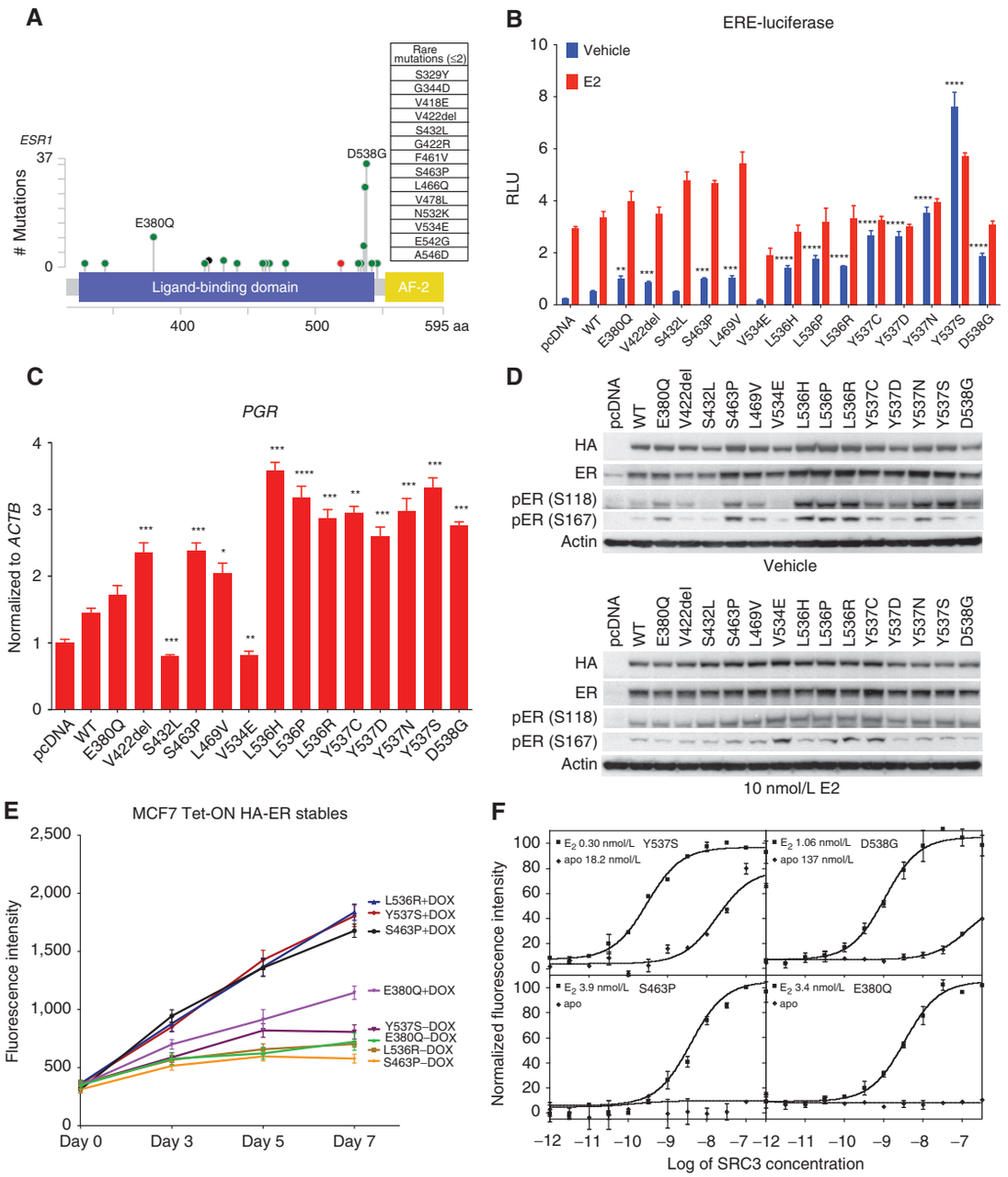

Figure 1. Newly detected *ESR1* mutations exhibit a range of estrogen-independent activities. **A,** Diagram of *ESR1* ligand-binding domain with somatic mutations identified from 929 breast tumors analyzed. Height of the circles correlates to the number of cases with that specific mutation. The color codes of the circles are as follows: green for missense mutations, red for truncating mutations (nonsense, nonstop, frameshift deletion, frameshift insertion, splice site) and black for in-frame mutations. AF-2, Activation function-2. **B,** Activation of ER reporter gene. ER$^+$ MCF7 cells were transfected with empty vector, HA-ERα WT or indicated *ESR1* mutation, estrogen response element (ERE)-luciferase and Renilla luciferase reporter constructs in hormone-depleted medium with 10 nmol/L of E2 added for 24 hours where indicated. Firefly luciferase activity shows increased activity in the absence of E2 or presence of E2 for certain mutations. Graphs were plotted with the mean ± SD of three biological replicates. *, $P < 0.05$; **, $P < 0.01$; ***, $P < 0.001$; ****, $P < 0.0001$. **C,** Activation of ER target genes. MCF7 cells were transfected with empty vector, HA-ERα WT or mutant in hormone-depleted medium and harvested 48 hours after transfection for qRT-PCR analysis. Bars represent mean ± SD of three technical replicates normalized to actin (ACTB) expression. *, $P < 0.05$; **, $P < 0.01$; ***, $P < 0.001$; ****, $P < 0.0001$. **D,** Activation of ER phosphorylation in MCF7 cells. Expression level of the mutant HA-tagged ERs and their relative phosphorylation status at Serine118 and Serine 167, treated with or without 10 nmol/L E2 for 24 hours by immunoblot analysis with specific antibodies as indicated. **E,** Activation of hormone-independent cell proliferation. Doxycycline-inducible ER-mutant receptors (E380Q, S463P, L536R, and Y537S) expressing MCF7 cells were seeded in 96-well plates in hormone-depleted medium with or without the addition of doxycycline and proliferation was assayed using resazurin reagent. Data show sufficiency of these four mutants to promote cell growth in the absence of estradiol. Each point in the graph represented mean ± SD of six technical replicates. **F,** Binding of the SRC3 nuclear receptor domain to Y537S, D538G, E380Q, or S463P ERα LBD in the absence or presence of E2. SRC3 was titrated into a fixed amount of ER-LBD-biotin and time-resolved Förster resonance energy transfer (tr-FRET) indicated that only Y537S and D538G were able to recruit SRC3 in the absence of E2 but not E380Q and S463P. LBD, ligand-binding domain.

liver and bone were the two most frequent, whereas none were detected in brain metastasis biopsies. The most frequent mutations in this series were D538G ($n = 34$), Y537S ($n = 13$), E380Q ($n = 20$), Y537C ($n = 6$), Y537N ($n = 5$), and L536H ($n = 4$). A number of other mutations were also observed at low frequency ($n \leq 2$), most of which have not previously been described (Supplementary Table S2). Although these individual mutations are not common, in aggregate they represent 20% of the cases of LBD mutations in *ESR1*.

The presence of a somatic mutation in the LBD of *ESR1* does not necessarily imply constitutive activity, and thus we sought to characterize the activity of a set of these infrequent mutants and compare them with the activities of the better-described variants such as Y537S. We generated hemagglutinin (HA)-tagged *ESR1* constructs with mutations introduced by site-directed mutagenesis and determined their activity through luciferase assays performed in the breast cancer cell lines MCF7 (ER^+) and SKBr3 (ER^-). First, to determine if the mutants had the ability to drive estrogen-independent transcription in the cellular context in which they are typically found (ER^+ breast cancer), we examined the ability of transient expression of mutant ER to promote transcription from an estrogen response element (ERE)-luciferase construct in MCF7 cells. We found that most of the mutant ERs had elevated ERE-luciferase activity in the absence of estradiol (E2) compared with WT ER, although none of them displayed activity higher than Y537S (Fig. 1B). There were two notable exceptions, however, in which the S432L and V534E mutants showed no increase in activity in the absence of E2, despite being expressed at relatively similar levels as that of WT (Supplementary Fig. S1A). In addition to the augmentation of E2-independent activity, we examined whether any of the mutants had altered response to E2. ER with mutations in amino acid 537 showed little further induction with the addition of estradiol, whereas all the other mutants, including S432L and V534E, showed induction with the addition of E2, as was the case for WT. Because the effect of E2 addition for these mutants could be ascribed to the presence of the endogenous WT ER, we also examined the effect of mutant ER expression in ER^- SKBr3 cells (Supplementary Fig. S1B). With the exception of Y537S, which is already maximally activated, the other ER mutants could be further activated by the addition of E2 in SKBr3 cells. This includes the S432L and V534E mutants, demonstrating that although these mutations are not constitutively active, they are also not inactivating alterations. The E2-independent activities of the ER mutants were not restricted to the luciferase reporter, as demonstrated by the induction of endogenous ER-dependent transcripts such as *PGR* and *GREB1* (Fig. 1C and Supplementary Fig. S1C). As observed with the luciferase assays, most of the mutants could induce transcripts to levels above that from WT in the absence of E2. Once again, the S432L and V534E mutants showed little evidence of constitutive activity in the absence of E2, whereas the ESR amino acid 536 and 537 mutants were the most active. In addition to regulating ER target genes directly through ER binding sites in the genome, ER modulates gene expression indirectly via interaction with other transcription factors, such as the activator protein-1 (AP1). We thus examined the effect of several ER mutants on the induction of AP1 target genes, namely *CCND1* and *MYC*, and found no significant changes in the levels of these two gene transcripts in comparing WT and mutant ERs (data not shown).

We looked for further evidence of biological activation of these somatic LBD mutants beyond assays for transcriptional activation. The phosphorylation of serine 118 and serine 167 of ER has been correlated with receptor activation in the absence of ligand (10–12). Consistent with the transcriptional assays, all mutants except S432L and V534E showed increased steady state ER S118 and S167 phosphorylation compared with WT in the absence of E2 when expressed in MCF7 cells (Fig. 1D). The addition of E2 suppressed apparent differences between phosphorylation of WT and most of the mutants (Fig. 1D). There were slight differences in the expression levels of ESR mutants (HA and ER blots) despite our efforts to achieve equal expression. This may be partly due to differential effects of some mutants on receptor stability, which we have demonstrated previously with Y537S and D538G (3). Together, these data demonstrate the constitutive activity of most of the infrequent *ESR1* mutations, and also reveal that at least two mutants (V534E and S432L) show no evidence of constitutive activation.

Given their constitutive activities, we hypothesized that these infrequent ER mutants might promote estrogen-independent tumor growth. We therefore generated doxycycline-inducible cell lines that expressed four representative ER mutants (E380Q, S463P, L536R, and Y537S) in the estrogen-dependent MCF7 model and examined their proliferation in estrogen-deprived medium. The concentrations of doxycycline used to induce comparable levels of ER expression were determined by immunoblot analyses and quantitative PCR (Supplementary Fig. S2A and S2B). We found that this set of mutants behaved similarly to Y537S in their ability to promote E2-independent growth (Fig. 1E). However, there were some differences observed in the degree of growth stimulation, such as the E380Q mutant promoting growth to a lesser degree than the other mutants. Overall, the data point to several infrequent LBD mutants driving higher estrogen-independent receptor activity and thereby potentially promoting resistance to estrogen deprivation therapy.

The data together point to significant differences in the level of estrogen-independent activity of recurrent mutants with the well-characterized mutants in the loop between helix 11–12 (Y537S and D538G) being more potent inducers than some of the less frequent mutants (e.g., S463P or E380Q). One hallmark of both ligand-bound ER as well as constitutively active mutants such as Y537S is their ability to induce a conformation that binds coactivator proteins. To characterize whether these less frequent mutants could induce this "agonist conformation" *in vitro* without estradiol, we performed a time-resolved Förster Resonance Energy Transfer (tr-FRET) assay with steroid receptor coactivator 3 (SRC3) nuclear receptor domain (NRD) titrated to a fixed amount of mutant ER-LBD (Y537S, D538G, S463P, and E380Q; refs. 13, 14). SRC3 is a well-established ER coactivator that is highly expressed in breast cancer cells and has a high affinity for ligand-bound ER (15). As shown in Fig. 1F, SRC3 NRD bound to unliganded Y537S with the highest affinity (18.2 nmol/L). The D538G mutant was also able to bind SRC3 in the absence of E2 (137 nmol/L) albeit somewhat less avidly than Y537S. In contrast, no binding was detected

for S436P and E380Q LBD whatsoever in the absence of E2. When the ER mutants were presaturated with E2, all of them bound to SRC3 NRD with varying affinities. S463P and E380Q showed similar affinities (EC_{50} = 3.9 nmol/L and 3.4 nmol/L), whereas Y537S and D538G had higher affinities (EC_{50} = 0.3 nmol/L and 1.1 nmol/L). The results of a trypsin digestion FRET assay further demonstrated the differences between the conformations of the mutants. This assay tests accessibility of the region of surrounding K529 to trypsin access and cleavage. All mutants tested provide substantial to major conformational stabilization of this region, but there were significant differences between mutants (Supplementary Table S3). In the absence of ligand (Apo), the t½ of WT-ER is the shortest at 3 minutes, implying that this region of the WT-ER is very accessible to trypsin attack. In contrast, Y537S and S463P demonstrate the greatest stabilization, in the range of 15–25-fold, followed by D538G, E380Q, and L536R with less than 5-fold stabilization. In the presence of ligand, marked stabilization is provided by the same two mutations (Y537S and S463P), as well as by D538G compared with WT. Although the degree of stabilization provided by the mutations does not fully correlate with their degree of constitutive activity, it provides evidence that the conformations of the mutants, at least in the region of helix 11, are quite different. Altogether, the data are consistent with mutants inducing constitutive activity through distinctive mechanisms and with Y537S appearing to be the most active.

Efficacy of SERDs Against ER Mutants

Previous work has suggested that ER antagonists are able to inhibit ER mutants but may be less potent than they are against WT ER (3). Given the differential activities of the LBD mutants, we asked whether different LBD mutants had comparable activity against the pure ER antagonist, fulvestrant (ICI). We examined the effect of selected ER mutants upon the dose-dependent inhibition of ER-driven transcription and proliferation by fulvestrant in MCF7 cells. Fulvestrant was able to inhibit the activity of all of the mutants; however, it appeared that the Y537S mutants required significantly higher levels of drug (70-fold higher IC_{99} for Y537S compared with WT) to fully inhibit their activities (Fig. 2A). In contrast, E380Q and S463P showed only slight resistance to fulvestrant with 2-fold higher IC_{99} as compared with WT (Fig. 2B). In terms of cell proliferation, Y537S required the highest concentration of fulvestrant (IC_{50} = 55-fold higher than WT) for complete growth inhibition, whereas several other mutants had modest effects (Y537C/N/D, D538G, and S463P; Fig. 2C and D and Supplementary Fig. S3A–S3D). This result is fairly concordant with the data from Fig. 2A and B. One exception is that S463P mutant appeared to have a greater effect on fulvestrant sensitivity in the proliferation assay than the transcriptional assay. This is consistent with a greater impact of this mutant in promoting estrogen-independent proliferation than transcription (Fig. 1E and C). The differential effects of fulvestrant upon ER-driven transcription from different mutants were also evident by assessing *GREB1* and *PGR* transcript levels by quantitative PCR (Supplementary Fig. S3E and S3F). Taken together, the data indicate that certain *ESR1* mutants can alter fulvestrant sensitivity *in vitro*.

To test if the partial resistance conferred by ER mutants was a class effect for SERDs, we compared the effects of three other SERDs, namely AZD9496 (16), RU-58668, and GDC-0810, on the WT and mutant cell lines. Although all three SERDs were capable of inhibiting cell proliferation by all mutants, significantly higher concentrations were consistently required for Y537S (Supplementary Fig. S4A–S4F). These findings corroborate previously published reports where the Y537S mutation led to reduced rates of ligand association and greater resistance to disruption of ligand binding by urea compared with WT (17).

Because SERD potency was tested using a model involving transient expression of the mutants, we sought to confirm the findings regarding Y537S in a system in which the mutation was expressed from its endogenous genomic locus. We therefore generated an *ESR1* knock-in of Y537S into the MCF7 cell line, using CRISPR/Cas9-mediated genome editing. The insertion of Y537S into the *ESR1* gene locus was confirmed by digital droplet (dd) PCR analysis of the parental cells, pooled cells (cells before single-cell sorting), and Y537S CRISPR knock-in cells (clone B3). These data demonstrated that the knock-in cell line is homozygous for the Y537S mutation, having an insignificant number of WT positive droplets detected (Supplementary Fig. S5). Cells expressing the Y537S allele also demonstrated enhanced expression of progesterone receptor (PR) protein and proliferation in hormone-depleted media compared with parental cells (Fig. 2E and F). The potency of fulvestrant and AZD9496 in Y537S-expressing cells was examined by assaying cell proliferation over a range of drug doses. As shown in Fig. 2G, the growth of MCF7 WT cells was inhibited by fulvestrant and AZD9496 at an IC_{50} concentration of 0.4 nmol/L, whereas in the Y537S-expressing cells, fulvestrant and AZD9496 inhibited growth with an IC_{50} of 25 nmol/L (Fig. 2H). These reduced sensitivities in the CRISPR knock-in Y537S cell line are consistent with the results seen with the doxycycline-induced overexpression mutant cell lines.

Superior Antitumor Activity on ER Mutant–Expressing Xenografts Achieved with AZD9496

The poor pharmacokinetic properties of fulvestrant are well documented in both mice and humans (3, 18). Given the comparable efficacy of AZD9496 and fulvestrant *in vitro* and the high serum levels of AZD9496 achievable through oral administration, we sought to compare these drugs in xenograft models of ER-mutant disease. We examined xenografts from the MCF7 cells engineered to express WT or mutant ER under a doxycycline-inducible promoter (3). We have previously demonstrated that the growth of these tumors is entirely dependent on ER signaling and that complete ablation of ER is able to fully block tumor growth. Maximally effective doses of fulvestrant (200 mg/kg) twice weekly via subcutaneous injection or AZD9496 (15 mg/kg) orally once daily were administered to mice with tumors expressing WT, E380Q, S463P, Y537S, or D538G ER. Fulvestrant fully inhibited the growth of the WT-, E380Q-, and S463P-expressing tumors while nearly completely inhibiting the growth of D538G tumors (Fig. 3A–E). The Y537S-expressing tumors, however, continued to grow in the presence of fulvestrant, albeit more slowly than in untreated controls. Whereas fulvestrant was only partially effective at suppressing the

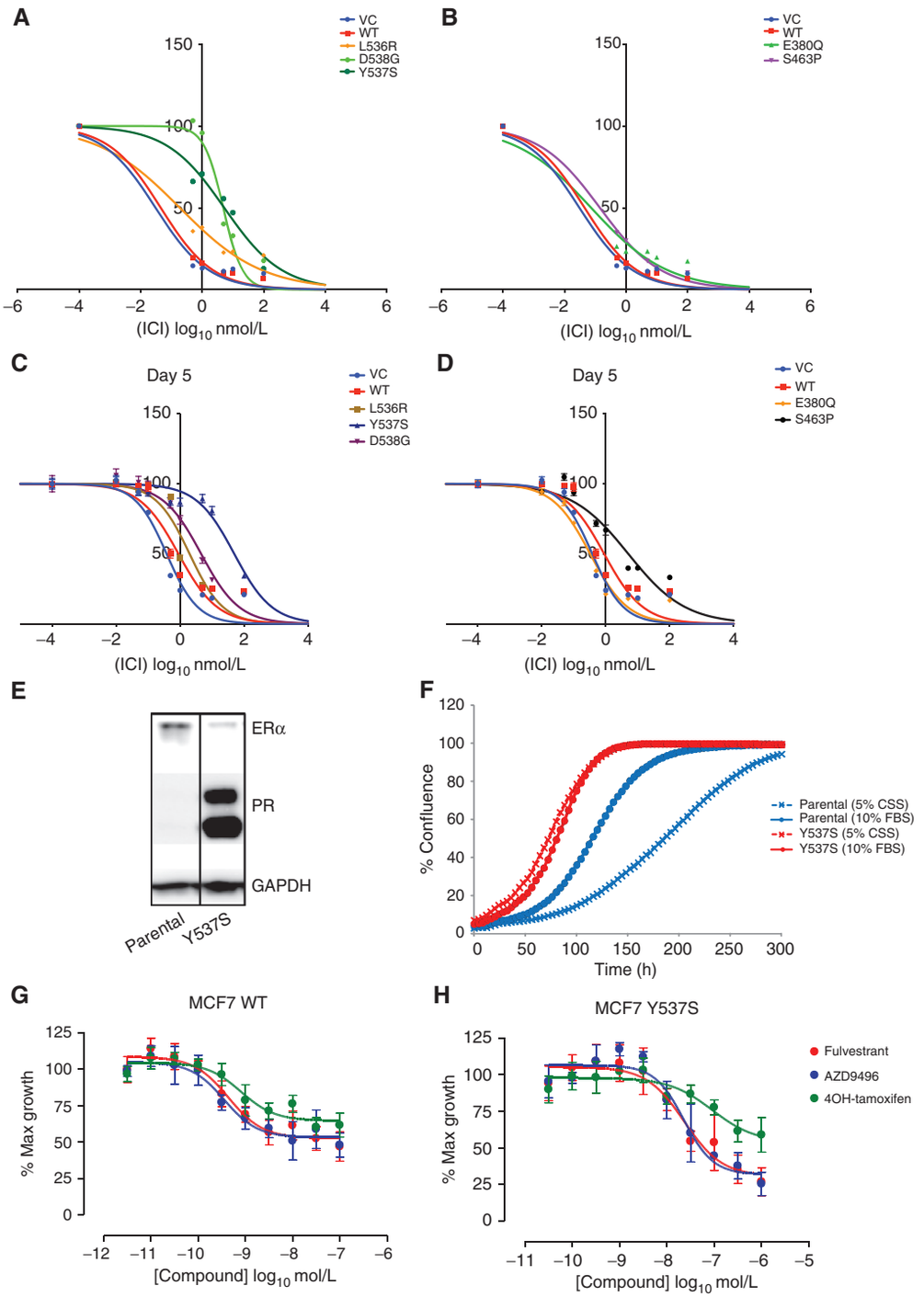

Figure 2. Efficacy of SERDs against ER mutants. Inhibition of WT and mutant-driven ERE luciferase (**A–B**) and proliferation (**C–D**) by fulvestrant (ICI). Doxycycline-induced WT and mutant ER-expressing MCF7 cells were treated with various doses of each antagonist in regular medium, demonstrating that the more active mutants required higher level of antagonists for complete inhibition. Graphs were plotted with the mean ± SD of two technical or six biological replicates respectively. (Note: SD values for Fig. 3A and B are too low for error bars to be visible in the graphs.) **E,** Detection of PR levels in MCF7 Y537S CRISPR knock-in cell by Western blot showed elevated PR levels in the Y537S knock-in cells in comparison with the parental line, indicating the expression of Y537S ER-mutant receptors. **F,** Proliferation assays of parental and Y537S CRISPR knock-in cell lines performed in hormone-depleted or regular media whereby Y537S knock-in cells showed estrogen-independent cell proliferation. **G** and **H,** Proliferation assays of parental MCF7 and MCF7 Y537S CRISPR knock-in cells treated with various doses of fulvestrant, AZD9496, or 4OHT demonstrated that significantly higher doses are required to cause growth inhibition of Y537S-expressing cells by ER antagonists. Cell confluency was measured using the IncuCyte Zoom standard software over a few days. Graphs were plotted with the mean ± SD of three biological replicates.

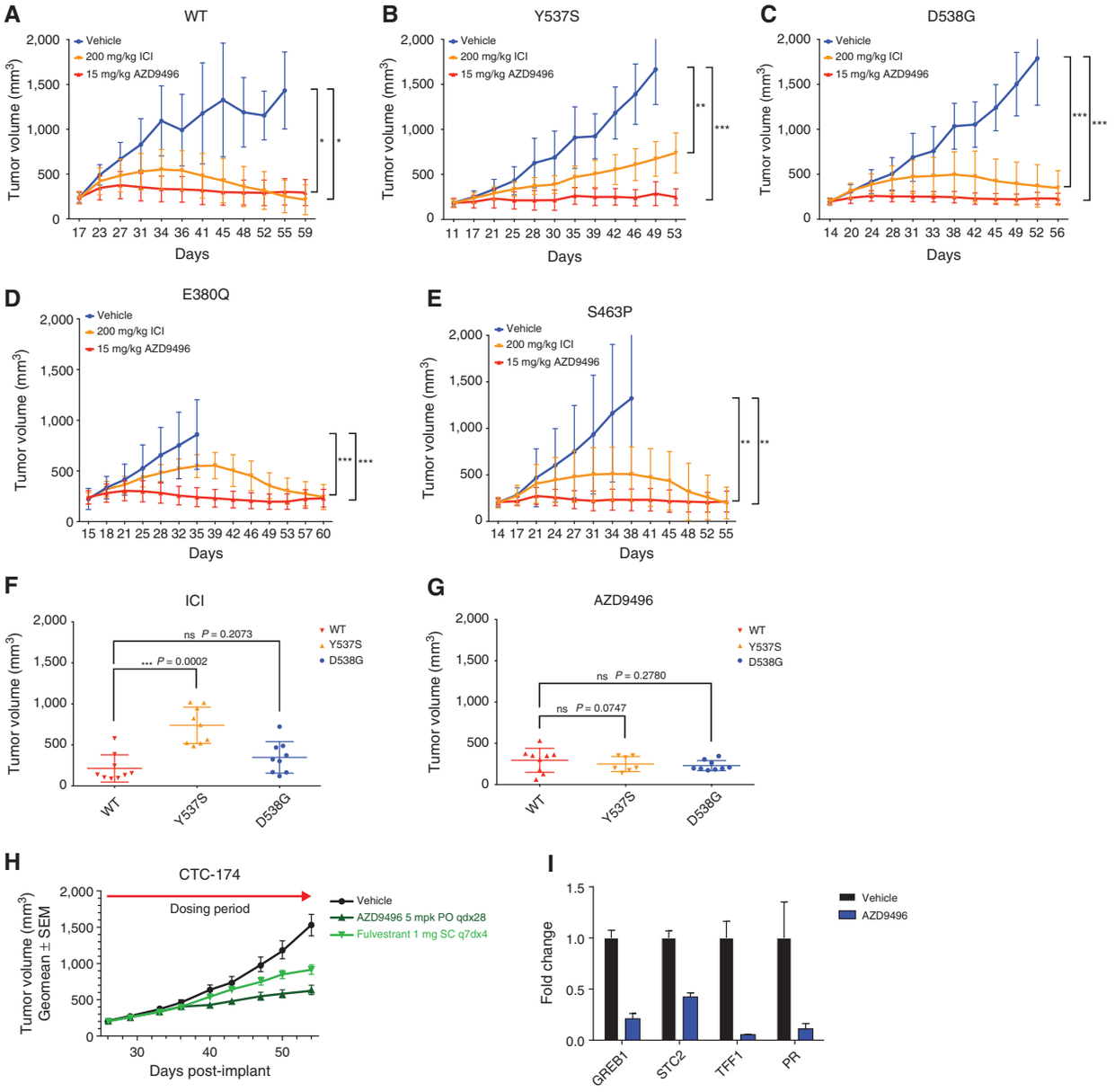

Figure 3. AZD9496 demonstrates superior antitumor effects on ER-mutant expressing xenografts. Mice bearing MCF7-inducible HA-ER WT (**A**), Y537S (**B**), D538G (**C**), E380Q (**D**), or S463P (**E**) tumors were randomly assigned to treatment groups of either 15 mg/kg of AZD9496 daily orally or 200 mg/kg of fulvestrant twice weekly, s.c. Tumors treated with AZD9496 showed greater growth inhibition as compared with those treated with fulvestrant. The result was presented as average tumor volume measured for each group ± SD ($n = 10$ mice/group). *, $P < 0.05$; **, $P < 0.01$; ***, $P < 0.001$; ****, $P < 0.0001$. **F** and **G,** Scatter plots of the volumes of tumors expressing WT, Y537S, or D538G treated with either fulvestrant (ICI) or AZD9496 taken at the end of the xenograft studies shown in **A–C**. T-tests comparing the volumes of mutant tumors with those of the WT indicated significant resistance of Y537S-mutant tumors to fulvestrant treatment. *, $P < 0.05$; **, $P < 0.01$; ***, $P < 0.001$; ****, $P < 0.0001$. **H,** PDX, CTC-174, with D538G mutation, showed greater growth arrest with 5 mg/kg of AZD9496. The result was presented as average tumor volume measured for each group ± SEM. **I,** Quantitative PCR detection of various ER target genes of AZD9496-treated CTC-174, the D538G PDX model, showed significant reduction in the transcript levels of *GREB1, STC2, TFF1*, and *PGR* when compared with the vehicle, indicating inhibition of the ER signaling pathway by AZD9496. Graphs were plotted with the mean ± SD of three technical replicates.

Y537S tumors, AZD9496 was able to completely inhibit their growth. The relative resistance of the Y537S tumors to fulvestrant was evident when we compared the sizes of the tumors at the end of the study by plotting them as scatter plots, which showed that the Y537S tumors were significantly larger than WT or D538G tumors in the fulvestrant arms (ICI) but not in the AZD9496 arms (Fig. 3F and G). In contrast, tumors expressing the alternate Y537 mutations, Y537C/N as well as V422del, responded similarly to WT upon inhibition by either fulvestrant or AZD9496 (Supplementary

Fig. S6A–S6D). Similar observations were made when we tested the effect of another bioavailable SERD, GDC-0810, on the growth of ER-mutant tumors, suggesting that the improved pharmacokinetic properties of the antagonists aid in efficient targeting of the mutant ER (Supplementary Fig. S7A–S7C).

As further support of the potential for ER antagonists to target most ER-mutant tumors, we examined the effect of AZD9496 and fulvestrant on the growth of a patient-derived xenograft (PDX), CTC-174 (19), that expresses a D538G *ESR1* mutation (Supplementary Fig. S8A and S8B). Both AZD9496 and fulvestrant were able to slow tumor growth in this model with a slightly enhanced efficacy seen for AZD9496 in this context, similar to what was observed for the MCF7-D538G model (Fig. 3H and C). It should be noted that unlike the MCF7 model, growth of this particular xenograft has never been shown to be fully dependent on ER signaling alone, and this may be partially affected by *PIK3CA*^{N345K} (activating mutation) and two *ARID1A* truncation mutations (E1776* and S705fs; inactivating mutations) identified in sequencing of this model. Consistent with these results, assessment of ER-driven transcripts in the AZD9496- and vehicle-treated tumors shows marked reduction of ER activity from AZD9496 administration, suggesting it was efficacious in blocking the ER-driven component of this disease (Fig. 3I). Overall, the data from the two ER mutant models are consistent with the ability of AZD9496 to inhibit mutant ER-driven tumor growth across a broader range of mutants than fulvestrant *in vivo*. In support of this, we examined the drug levels of AZD9496 and fulvestrant in serum using pharmacokinetic modeling. We found that the average area under the curve (AUC) and C_{max} for fulvestrant (AUC = 5.29 μmol/L · h, C_{max} = 0.65 μmol/L) were markedly lower than those obtained for AZD9496 (AUC = 218 μmol/L · h, C_{max} = 59 μmol/L). This difference was observed despite dosing fulvestrant at levels approximately 5-fold higher than are administered to patients. Taken together, the data are consistent with fulvestrant and AZD9496 both inhibiting mutant ER activities *in vitro* but AZD9496 having superior pharmacokinetic properties enabling *in vivo* efficacy across a broader range of ER-mutant models, including those driven by Y537S.

DISCUSSION

The two major strategies for therapeutic targeting of hormonal signaling in breast cancer are estrogen deprivation and direct antagonism of the estrogen receptor. Through large clinical investigations, estrogen deprivation has become the clinical standard for both the adjuvant and metastatic setting. Recently, however, resistance to estrogen deprivation therapy has been characterized as frequently involving activating mutations in the estrogen receptor (20). Biochemical and structural studies of the most common mutations have shown them to promote an activated conformation in the absence of ligand. This conformation remains permissive for ligand binding, thus leading to the hypothesis that direct antagonism may be a rational strategy for these mutant receptors. However, the ability of different ER antagonists to effectively block all of the different ER mutants that occur in the clinic has not been established. In this study, we characterize the diversity of activating *ESR1* mutations that are observed in the clinic and determine conditions needed for ER antagonists to be effective against the mutations.

Initial reports on the existence of somatic *ESR1* mutations in ER$^+$ MBC came from somewhat smaller populations of tumors in the range of 11 to 76 tumors (3–6). Recurrent alterations were the focal point of the *in vitro* characterizations, and it was demonstrated that the mutations D538G, Y537S/N/C, and L536R all promoted estrogen-independent activation of the receptor (3–6). In addition, several of these reports assessed the ability of ER antagonists such as 4-hydroxytamoxifen and fulvestrant to block these mutant receptors (3–6). From these data, it appeared that the mutant receptors might be inhibited, albeit at higher drug concentrations (3, 4, 6, 21). Whether all *ESR1* mutants followed the pattern of these mutations in amino acids 536 to 538 was unknown. In the current study, we report the identification of *ESR1* LBD mutations from a large cohort of patients with MBC. The majority of mutations are in amino acids 538, 537, 380, and 536. However, we detected a number of low-frequency novel mutations, which collectively comprised 20% of the mutations detected within this series. An analysis of the different mutations revealed a range of activities. Across a variety of assays surveying *in vitro* conformation, phosphorylation, transcriptional activity, and estrogen-independent proliferation, the Y537S mutant appeared to have the greatest effect. Mutation in neighboring residues 536 and 538 also led to high activity; however, in both cases, these were often at or below the level observed with estradiol stimulation. It is also notable that mutation at the same amino acid 537 site to cysteine (C), aspartic acid (D), and asparagine (N) caused receptor activation, but to a lesser degree than did the S mutant. Hence, the level of ER activation depends on both the site of mutation and the nature of the mutant residue. Beyond these mutations, all of the mutants outside this region show only modest activity in the absence of estradiol. In addition, two somatic mutations (S432L and V534E) showed no activation in the absence of estrogen and so their role in promoting resistance to aromatase inhibition is not supported by these data. The basis for these differences in basal activation levels is likely to lie in the conformational changes that these mutations induce. Structures of D538G and Y537S ligand binding domains have now been reported and show similarities in the mechanisms whereby they induce ligand-independent activation (22). However, even these two structures highlight important differences in hydrogen bonding and side chain packing that may well translate into the apparent differences in coactivator binding affinity and basal transcriptional activity. Alterations such as E380Q or S463P appear likely to promote hormone independence through still other mechanisms as evidenced by the lack of coactivator binding they induce *in vitro* in the absence of estradiol. These findings support ongoing efforts to characterize structures of all of the different recurrent ER mutants as they likely reveal the different constraints that prevent unliganded ER from activating transcription.

From a translational perspective, the varying activities observed from different *ESR1* mutations raise several issues. First, it is not yet clear whether different mutations are more or less able to promote resistance to aromatase inhibitors. The data revealing the presence of *ESR1* mutations in hormone-independent tumors and their association with poor

outcomes have largely been obtained from small populations that are underpowered to look for differences in outcome due to different mutations. One recent report suggested that patients with D538G and Y537S mutant tumors may have slight differences in survival outcomes, but this again involved numbers too small to be conclusive on this point (20). Our data raise the possibility that some mutations may indeed be more effective in promoting resistance than others. Perhaps of even greater significance, estrogen receptor antagonists might have differential efficacies as a function of mutation type and activity, a possibility that we have investigated in our models.

Estrogen receptor antagonists such as fulvestrant appear broadly effective against ER mutants *in vitro*, but important differences emerge when comparing the potencies against individual mutants. Whereas several mutations had a modest effect on fulvestrant efficacy, Y537S led to major changes in the concentration required to fully inhibit ER activities. What accounts for the specific differences in drug potency is not yet clear, but it is notable that the Y537S mutant is the most activated in the absence of ligand and also shows reduced ligand association rates and binding affinities *in vitro*. Perhaps this points to a particularly active state of the receptor that might be targeted by a unique pharmacologic strategy. However, despite this reduced affinity, antagonists such as fulvestrant can ultimately inhibit ER mutants, including Y537S, *in vitro*, albeit at higher doses. To address whether these differences in potency might have clinical implications, we examined the *in vivo* effects of these drugs in xenograft models.

Using these models, we found that fulvestrant was capable of fully inhibiting WT, E380Q, and S463P ER-driven breast cancers. However, Y537S mutants were not fully inhibited by fulvestrant despite dosing to higher levels than are typically achieved in the clinic. The tumor model driven by D538G was nearly completely inhibited by fulvestrant and so appeared to behave more like the E380Q and S463P mutants *in vivo*. The oral SERDs, AZD9496 and GDC-0810, were able to completely block growth of WT and all mutant ER-driven models including those driven by Y537S. These findings are consistent with clinical observations that the major limitation of fulvestrant is its poor pharmacokinetic properties. Although fulvestrant is highly potent *in vitro*, receptor occupancy *in vivo* is incomplete at the steady-state serum concentrations reached with current dosing (18). However, higher peak and steady-state levels of AZD9496 and GDC-0810 are achievable despite administering significantly less drug to mice. As several more bioavailable SERDs such as AZD9496 and GDC-0810 are now in early clinical trial testing, the value of higher drug levels can be formally evaluated. Our data indicate the need to include assessment of specific mutations in this evaluation because mutations in amino acid 537 and perhaps also 536 and 538 will likely necessitate higher drug levels to achieve complete inhibition.

Finally, it is notable that the PDX model we analyzed demonstrated only partial tumor growth inhibition with AZD9496. Although the data for *ESR1* mutations are consistent with these alterations being common and reducing tumor dependence on estrogen, they do not imply that all mutant tumors are exclusively dependent on ER signaling for their growth. Tumor genotyping of *ESR1*-mutant breast cancers also reveals recurrent alterations in the PI3K/AKT pathway, cyclin D1, and FGF receptors, among others (3). These alterations likely reduce tumor dependence on ER signaling. Such tumors are appropriate candidates for combinations of antiestrogens with inhibitors of PI3K, AKT, CDK4/6, and FGFRs that are all in phase II/III testing. Our data suggest that the specific hormonal drug used in such a combination is likely to matter significantly, a point further emphasized by our recent observation that inhibition of growth signals such as PI3K/AKT led to further activation of and restored dependence upon ER signaling (23). Taken together, our data and the emerging literature suggest that more potent and bioavailable compounds to block ER signaling may play a key role in the management of ER^+ MBC.

METHODS

Reagents

17β-estradiol (E2) and RU-58668 were from Sigma-Aldrich and Tocris Bioscience (R&D Systems), respectively. All the drugs were dissolved in DMSO. AZD9496 and fulvestrant were kindly provided by AstraZeneca UK Limited. GDC-0810 was a kind gift from Seragon Pharmaceuticals Inc. Hemagglutinin (HA)-tag (Cat. No: 2367/Clone: 6E2), Progesterone receptor A/B (Cat. No: 8757S/Clone: D8Q2J) and anti–β-Actin (Cat. No: 4970S/Clone: 13E5) antibodies were purchased from Cell Signaling Technology.

Cell Culture

All cell lines were maintained at 37°C and 5% CO_2 in humidified atmosphere. The SKBr3 cell line was a kind gift from Dr. Neal Rosen (MSKCC). MCF7 Tet-On was obtained from Clontech in February 2013 and MCF7 was obtained from DSMZ in 2012. SKBr3 cells were grown in DMEM/F12 supplemented with 10% FBS, 100 μg/mL penicillin, 100 mg/mL streptomycin, and 4 mmol/L glutamine, and MCF7 Tet-On were grown in DMEM/F12 supplemented with 10% Tet System Approved FBS (Clontech), 100 μg/mL penicillin, 100 mg/mL streptomycin, 4 mmol/L glutamine, and 100 μg/mL of G418. MCF7 cells were cultured in phenol red-free RPMI-1640 media (Sigma, R7509) supplemented with 10% heat-inactivated fetal calf serum (FCS) or 5% charcoal/dextran-treated serum (CSS) to deplete hormones, 2 mmol/L L-glutamine (Corning). All cell lines were tested negative for *Mycoplasma* and authenticated by short-tandem repeat (STR) analysis in 2013.

Generation of Y537S CRISPR Knock-In Cell Lines

MCF7 cells were transfected with a single-guide RNA Cas9 vector and a donor cassette as a nondigested plasmid at a 2:1 ratio using Fugene (Promega). The guide RNA sequence used was ctccagcagcaggtcataga. The donor cassette contained a 800-bp and 1-kb homology regions for incorporation of the Y537S mutation via homologous directed repair (HDR). Between the homology regions, a Neomycin resistance gene was encoded, which was under the PKG promoter and used for selection of HDR events 48 hours after transfection. After two weeks of selection, single-cell clones were generated and screened with ddPCR for evidence of Y537S mutation. The ddPCR was performed (24) using ddPCR primers (cgggttggctctaaagtagt and aatgcgatgaagtagagccc) and specific probes (BHQ_cc{C}ctc{tAt}gacc{t}g_HEX and BHQ_CC{A}CTC{TCT}GAC{C}TG_FAM). The location of the insertion was confirmed using junction PCR with the following primer pairs:

1 (TTAGATCATGCTGTAGGCCCTG) + 2 (CTGGAACCCA TGAC CGGAAAG),
3 (GCAGATCCAGGGGGCATTTA) + 4 (GATGTGGAATGT GTGC GAGC),
2 (CTGGAACCCATGACCGGAAAG) 5 (GGATCAATTCTCT AGAG CTCGC).

Tide analysis (25) was used to confirm the frameshift mutation of the second *ESR1* allele. Targeted locus amplification (TLA) sequencing (26) confirmed the genotype of the 3 *ESR1* alleles (A2942C Y537S knock-in, inactivating single-base insertion knock-out, and inactivating 48-bp deletion).

PDXs

The CTC-174 PDX model was derived from patient circulating tumor cell (CTC) cultures, consent obtained according to the Human Biological Samples Policy, and purchased from Conversant Biologics. The CTCs were obtained from a 63-year-old patient with stage IV ER^+ breast cancer after 42 days of fulvestrant therapy and 26 days of eribulin therapy. To generate the PDX, EpCAM+CD44+ cells were suspended in PBS mixed with high-concentration Matrigel (BD Biosciences) at 10 mg/mL and ~650 cells were injected into the third mammary fat pad of a NOD/SCID (Cg-Prkdcscid Il2rgtm1Wjl/SzJ) mouse. In the tumor transplantation study, 2 × 2 mm pieces of tumor tissue from CTC-derived tumor xenografts were implanted in the mammary fad pad of Beige Nude XID mice. All procedures were performed in accordance with U.S. federal, state, and institutional guidelines in a facility accredited by the Association for Assessment and Accreditation of Laboratory Animal Care International. Tumor growth was calculated weekly by bilateral caliper measurement (length × width) and mice randomized into vehicle or treatment groups with approximate mean start size of 0.2 to 0.4 cm^3 for efficacy studies or 0.5 to 0.8 cm^3 for PD studies. Mice were dosed once daily by oral gavage or subcutaneous (s.c.) injection for fulvestrant at the times and doses indicated for the duration of the treatment period. Tumor growth inhibition from start of treatment was assessed by comparison of the mean change in tumor volume for the control and treated groups.

Animal Studies

Six-to-8-week-old nu/nu athymic BALB/c female mice were obtained from Harlan Laboratories, Inc., and maintained in pressurized ventilated caging. All studies were performed in compliance with institutional guidelines under an Institutional Animal Care and Use Committee–approved protocol (MSKCC#12-10-016). MCF7-inducible HA-ER xenograft tumors were established in nude mice by subcutaneously implanting 0.18-mg sustained release 17β-estradiol pellets with a 10 g trocar into one flank followed by injecting 1 × 10^7 cells suspended 1:1 (volume) with reconstituted basement membrane (Matrigel, Collaborative Research) on the opposite side 3 days afterward. When the tumors reached a size of ~200 mm^3, the mice bearing tumors from each cell line were randomized into 3 treatment groups, fed with water containing 0.2 to 0.5 mg/mL of doxycycline (0.2 mg/mL for WT, 1.0 mg/mL for E380Q, 0.1 mg/mL for S463P and 0.5 mg/mL for vector control, Y537S and D538G, respectively) and 0.1% sucrose for induction of ER expression, 24 hours before being treated with vehicle, 200 mg/kg of fulvestrant subcutaneously twice a week or 15 mg/kg of AZD9496 via gavage once daily. Tumor dimensions were measured with vernier calipers and tumor volumes calculated [$\pi/6 \times$ larger diameter × (smaller diameter)^2]. In this study, there was no blinding of the investigator as randomization of animals was done. Based upon our previous work measuring the variability in size and growth of MCF7 xenografts, we estimated 10 mice/group would allow us to detect tumor size differences of >200 mm^3.

Sequencing of Tumor Biopsies in the MSK-IMPACT Series

Study Population. All the patients were enrolled in an institution-wide Institutional Review Board–approved umbrella protocol allowing us to perform genomic testing on their tumors. Informed consent was obtained from all participating patients. This study was conducted in accordance with the Declaration of Helsinki. Between April 2014 and June 2015, 929 patients with confirmed metastatic breast carcinoma (631 with ER^+/$HER2^-$ disease) underwent MSK-IMPACT testing (27). Detailed clinical information including treatment exposures and subsequent clinical outcomes were collected from all patients.

DNA Extraction. Fifteen to 20 unstained 10 μm–thick formalin-fixed paraffin-embedded sections were obtained and microdissected to ensure >85% tumor content. DNA was extracted using the QIAamp DNA Micro Kit (Qiagen) and standard protocols. Mononuclear cells from peripheral blood were used to extract patient-matched normal DNA.

Sequencing. Deep sequencing of targeted genes was performed utilizing the MSK-IMPACT assay (27). Briefly, MSK-IMPACT is a targeted sequencing assay that involves hybridization of barcoded libraries to custom oligonucleotides (Nimblegen SeqCap) designed to capture all protein-coding exons and select introns of 410 commonly implicated oncogenes, tumor suppressor genes, and members of pathways deemed actionable by targeted therapies. The captured pool was sequenced on an Illumina HiSeq 2500 as 2 × 100 bp paired-end reads, resulting in approximately 500- to 1,000-fold coverage per tumor.

Please refer to the Supplementary Methods for the rest of the methods mentioned in the article.

Disclosure of Potential Conflicts of Interest

S. Chandarlapaty reports receiving commercial research support from Novartis and is a consultant/advisory board member for AstraZeneca. No potential conflicts of interest were disclosed by the other authors.

One of the Editors-in-Chief is an author on this article. In keeping with the AACR's editorial policy, the peer review of this submission was managed by a senior member of *Cancer Discovery*'s editorial team; a member of the AACR Publications Committee rendered the final decision concerning acceptability.

Authors' Contributions

Conception and design: W. Toy, J. Baselga, S. Chandarlapaty
Development of methodology: W. Toy, M. Lawson, K.E. Carlson, Z. Li, J.A. Katzenellenbogen, J. Baselga, S. Chandarlapaty
Acquisition of data (provided animals, acquired and managed patients, provided facilities, etc.): W. Toy, H. Weir, P. Razavi, M. Lawson, A.U. Goeppert, A.M. Mazzola, C. Morrow, W.L. Wong, E. De Stanchina, K.E. Carlson, T.S. Martin, Z. Li, J.A. Katzenellenbogen, S. Chandarlapaty
Analysis and interpretation of data (e.g., statistical analysis, biostatistics, computational analysis): W. Toy, H. Weir, P. Razavi, M. Lawson, A.U. Goeppert, A. Smith, J. Wilson, K.E. Carlson, T.S. Martin, Z. Li, J.A. Katzenellenbogen, J. Baselga, S. Chandarlapaty
Writing, review, and/or revision of the manuscript: W. Toy, H. Weir, P. Razavi, A.U. Goeppert, K.E. Carlson, T.S. Martin, J.A. Katzenellenbogen, G. Greene, J. Baselga, S. Chandarlapaty
Administrative, technical, or material support (i.e., reporting or organizing data, constructing databases): W. Toy, P. Razavi, M. Lawson, S. Uddin, J. Baselga, S. Chandarlapaty
Study supervision: S. Fanning, J. Baselga, S. Chandarlapaty

Acknowledgments

The authors thank Kinisha Gala, Allison Smith, and Neal Rosen for their insightful comments on the manuscript, and Marcello Maresca for the design and generation of the reagents used for the production of the Y537S *ESR1* MCF7 cell line.

Grant Support

S. Chandarlapaty and G. Greene are supported by a Department of Defense Breast Cancer Research Project Grant (W81XWH-14-1-0359).

S. Chandarlapaty is also supported by funds from Susan G. Komen and the Breast Cancer Research Foundation. The Marie-Josée and Henry R. Kravis Center for Molecular Oncology as well as an NCI Cancer Center Support Grant (CCSG, P30 CA08748) supported genomic sequencing. W. Toy was supported by an MSKCC Translational Research Oncology Training Fellowship made possible by the generous contribution of First Eagle Investment Management.

Received December 23, 2015; revised December 8, 2016; accepted December 14, 2016; published OnlineFirst December 16, 2016.

REFERENCES

1. Early Breast Cancer Trialists' Collaborative G. Effects of chemotherapy and hormonal therapy for early breast cancer on recurrence and 15-year survival: an overview of the randomised trials. Lancet 2005;365:1687–717.
2. Mouridsen H, Gershanovich M, Sun Y, Perez-Carrion R, Boni C, Monnier A, et al. Phase III study of letrozole versus tamoxifen as first-line therapy of advanced breast cancer in postmenopausal women: analysis of survival and update of efficacy from the International Letrozole Breast Cancer Group. J Clin Oncol 2003;21:2101–9.
3. Toy W, Shen Y, Won H, Green B, Sakr RA, Will M, et al. ESR1 ligand-binding domain mutations in hormone-resistant breast cancer. Nat Genet 2013;45:1439–45.
4. Robinson DR, Wu YM, Vats P, Su F, Lonigro RJ, Cao X, et al. Activating ESR1 mutations in hormone-resistant metastatic breast cancer. Nat Genet 2013;45:1446–51.
5. Merenbakh-Lamin K, Ben-Baruch N, Yeheskel A, Dvir A, Soussan-Gutman L, Jeselsohn R, et al. D538G mutation in estrogen receptor-alpha: a novel mechanism for acquired endocrine resistance in breast cancer. Cancer Res 2013;73:6856–64.
6. Jeselsohn R, Yelensky R, Buchwalter G, Frampton G, Meric-Bernstam F, Gonzalez-Angulo AM, et al. Emergence of constitutively active estrogen receptor-alpha mutations in pretreated advanced estrogen receptor-positive breast cancer. Clin Cancer Res 2014;20:1757–67.
7. Li S, Shen D, Shao J, Crowder R, Liu W, Prat A, et al. Endocrine-therapy-resistant ESR1 variants revealed by genomic characterization of breast-cancer-derived xenografts. Cell Rep 2013;4:1116–30.
8. Zhang QX, Borg A, Wolf DM, Oesterreich S, Fuqua SA. An estrogen receptor mutant with strong hormone-independent activity from a metastatic breast cancer. Cancer Res 1997;57:1244–9.
9. Nettles KW, Bruning JB, Gil G, Nowak J, Sharma SK, Hahm JB, et al. NFkappaB selectivity of estrogen receptor ligands revealed by comparative crystallographic analyses. Nat Chem Biol 2008;4:241–7.
10. Kato S, Endoh H, Masuhiro Y, Kitamoto T, Uchiyama S, Sasaki H, et a. Activation of the estrogen receptor through phosphorylation by mitogen-activated protein kinase. Science 1995;270:1491–4.
11. Le Goff P, Montano MM, Schodin DJ, Katzenellenbogen BS. Phosphorylation of the human estrogen receptor. Identification of hormone-regulated sites and examination of their influence on transcriptional activity. J Biol Chem 1994;269:4458–66.
12. Joel PB, Smith J, Sturgill TW, Fisher TL, Blenis J, Lannigan DA. pp90rsk1 regulates estrogen receptor-mediated transcription through phosphorylation of Ser-167. Mol Cell Biol 1998;18:1978–84.
13. Tamrazi A, Carlson KE, Rodriguez AL, Katzenellenbogen JA. Coactivator proteins as determinants of estrogen receptor structure and function: spectroscopic evidence for a novel coactivator-stabilized receptor conformation. Mol Endocrinol 2005;19:1516–28.
14. Jeyakumar M, Carlson KE, Gunther JR, Katzenellenbogen JA. Exploration of dimensions of estrogen potency: parsing ligand binding and coactivator binding affinities. J Biol Chem 2011;286:12971–82.
15. Liao L, Kuang SQ, Yuan Y, Gonzalez SM, O'Malley BW, Xu J. Molecular structure and biological function of the cancer-amplified nuclear receptor coactivator SRC-3/AIB1. J Steroid Biochem Mol Biol 2002;83:3–14.
16. De Savi C, Bradbury RH, Rabow AA, Norman RA, de Almeida C, Andrews DM, et al. Optimization of a novel binding motif to (E)-3-(3,5-Difluoro-4-((1R,3R)-2-(2-fluoro-2-methylpropyl)-3-methyl-2,3,4,9-tetra hydro-1H-pyrido[3,4-b]indol-1-yl)phenyl)acrylic Acid (AZD9496), a potent and orally bioavailable selective estrogen receptor downregulator and antagonist. J Med Chem 2015;58:8128–40.
17. Carlson KE, Choi I, Gee A, Katzenellenbogen BS, Katzenellenbogen JA. Altered ligand binding properties and enhanced stability of a constitutively active estrogen receptor: evidence that an open pocket conformation is required for ligand interaction. Biochemistry 1997;36:14897–905.
18. van Kruchten M, de Vries EG, Glaudemans AW, van Lanschot MC, van Faassen M, Kema IP, et al. Measuring residual estrogen receptor availability during fulvestrant therapy in patients with metastatic breast cancer. Cancer Discov 2015;5:72–81.
19. Weir HM, Bradbury RH, Lawson M, Rabow AA, Buttar D, Callis RJ, et al. AZD9496: an oral estrogen receptor inhibitor that blocks the growth of ER-positive and ESR1-mutant breast tumors in preclinical models. Cancer Res 2016;76:3307–18.
20. Chandarlapaty S, Chen D, He W, Sung P, Samoila A, You D, et al. Prevalence of ESR1 mutations in cell-free DNA and outcomes in metastatic breast cancer: a secondary analysis of the BOLERO-2 clinical trial. JAMA Oncol 2016;2:1310–5.
21. Wardell SE, Ellis MJ, Alley HM, Eisele K, VanArsdale T, Dann SG, et al. Efficacy of SERD/SERM Hybrid-CDK4/6 inhibitor combinations in models of endocrine therapy-resistant breast cancer. Clin Cancer Res 2015;21:5121–30.
22. Fanning SW, Mayne CG, Dharmarajan V, Carlson KE, Martin TA, Novick SJ, et al. Estrogen receptor alpha somatic mutations Y537S and D538G confer breast cancer endocrine resistance by stabilizing the activating function-2 binding conformation. eLife 2016;5. pii: e12792. doi: 10.7554/eLife.12792. [Epub ahead of print].
23. Bosch A, Li Z, Bergamaschi A, Ellis H, Toska E, Prat A, et al. PI3K inhibition results in enhanced estrogen receptor function and dependence in hormone receptor-positive breast cancer. Sci Transl Med 2015;7:283ra51.
24. Pinheiro LB, Coleman VA, Hindson CM, Herrmann J, Hindson BJ, Bhat S, et al. Evaluation of a droplet digital polymerase chain reaction format for DNA copy number quantification. Anal Chem 2012;84:1003–11.
25. Brinkman EK, Chen T, Amendola M, van Steensel B. Easy quantitative assessment of genome editing by sequence trace decomposition. Nucleic Acids Res 2014;42:e168.
26. de Vree PJ, de Wit E, Yilmaz M, van de Heijning M, Klous P, Verstegen MJ, et al. Targeted sequencing by proximity ligation for comprehensive variant detection and local haplotyping. Nat Biotechnol 2014;32:1019–25.
27. Cheng DT, Mitchell TN, Zehir A, Shah RH, Benayed R, Syed A, et al. Memorial Sloan Kettering-integrated mutation profiling of actionable cancer targets (MSK-IMPACT): a hybridization capture-based next-generation sequencing clinical assay for solid tumor molecular oncology. J Mol Diagn 2015;17:251–64.